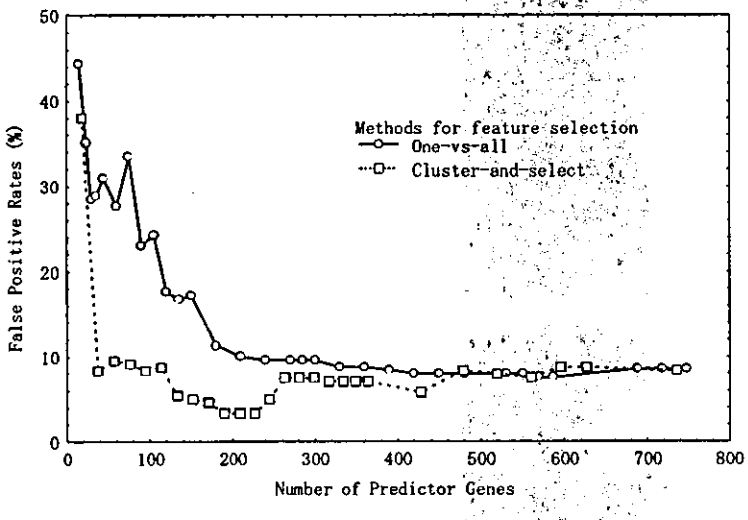

Figure 1: False positive error rates using different feature selection methods. Prototype matching (PM) algorithm is found to be more reliable using a gene set produced by the cluster-and-select method.

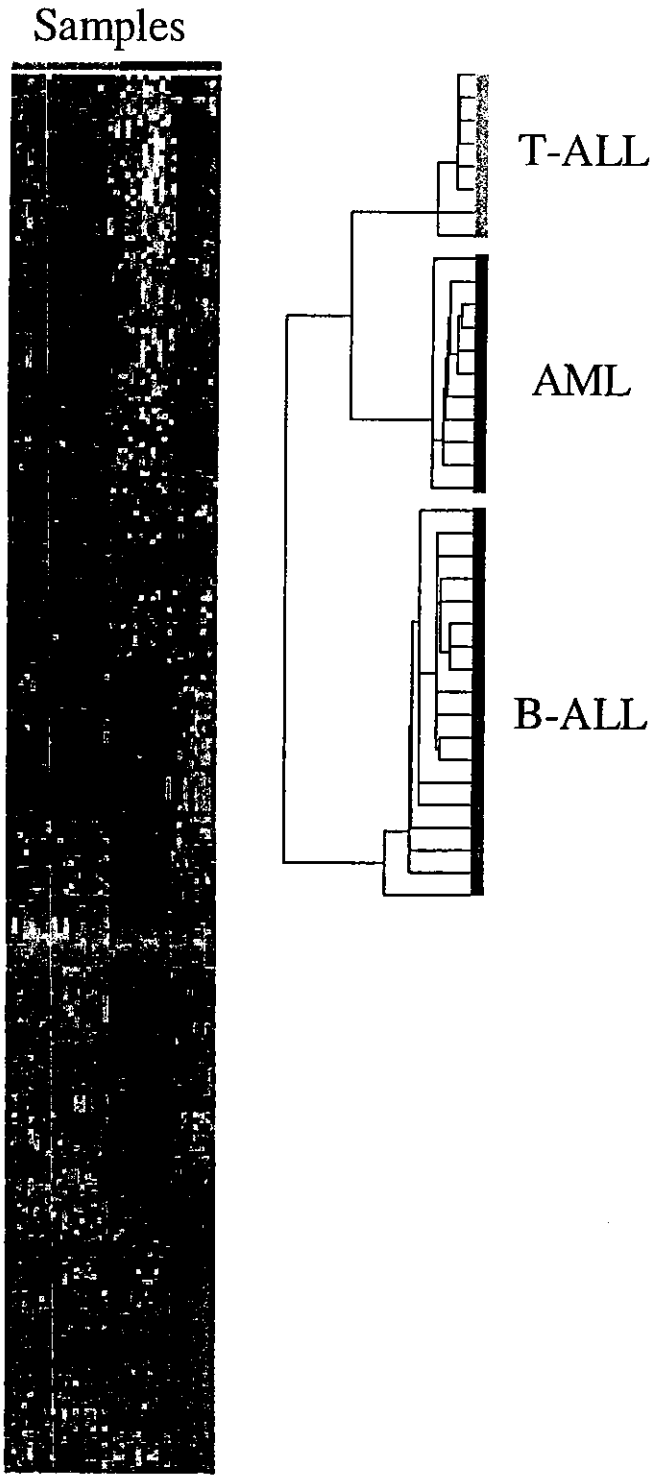

Figure 2: A set of 227 gense chosen for classification of B-cell acute lymphoblastic leukemia (B-ALL), T-cell acute lymphoblastic leukemia (T-ALL), and acute myeloid leukemia (AML)[1]. Instead of searching the whole gene list for predefined expression patterns, we try to find all existing patterns that could be helpful in cancer classification. Red indicates high expression and green low expression. A list of gene names is given in the supplementary information.

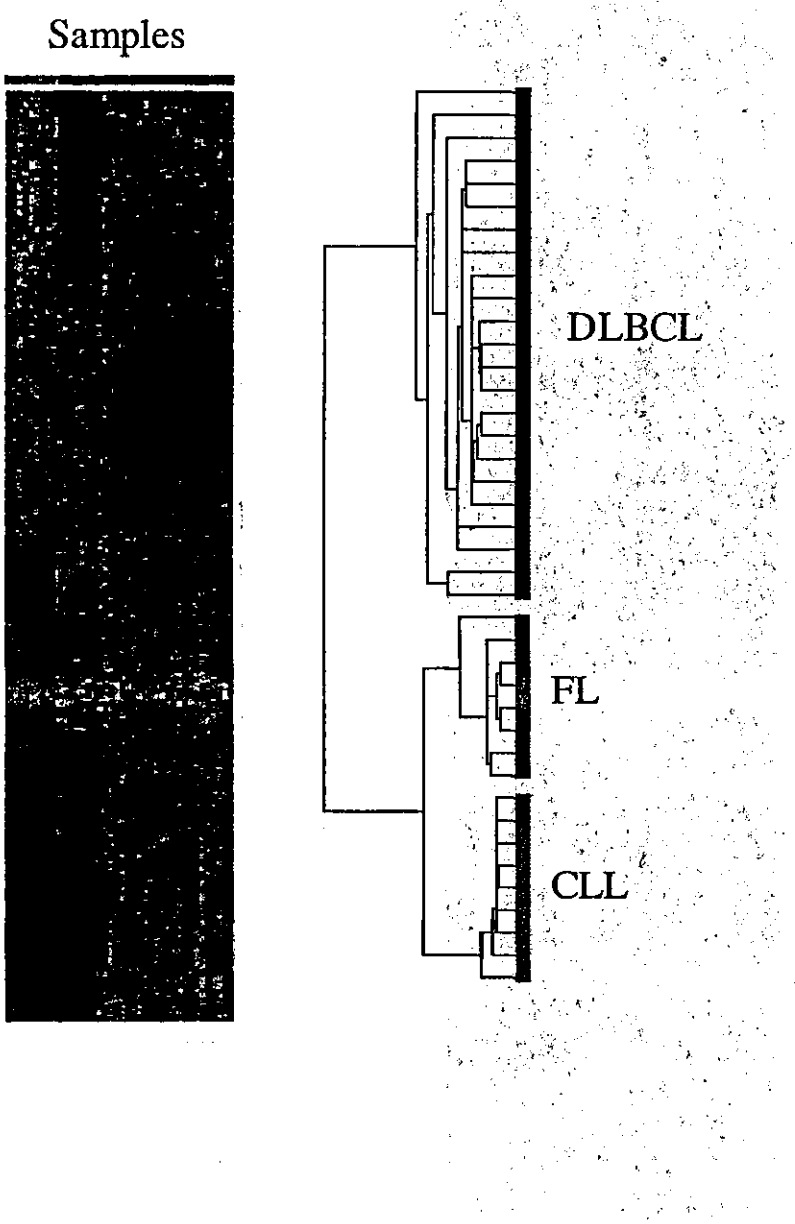

Figure 3: Predictor genes for the lymphoma dataset[4] containing three subtypes, namely, diffuse large B-cell lymphoma (DLBCL), follicular lymphoma (FL), and chronic lymphocytic leukemia (CLL). A list of gene names is given in the supplementary information.

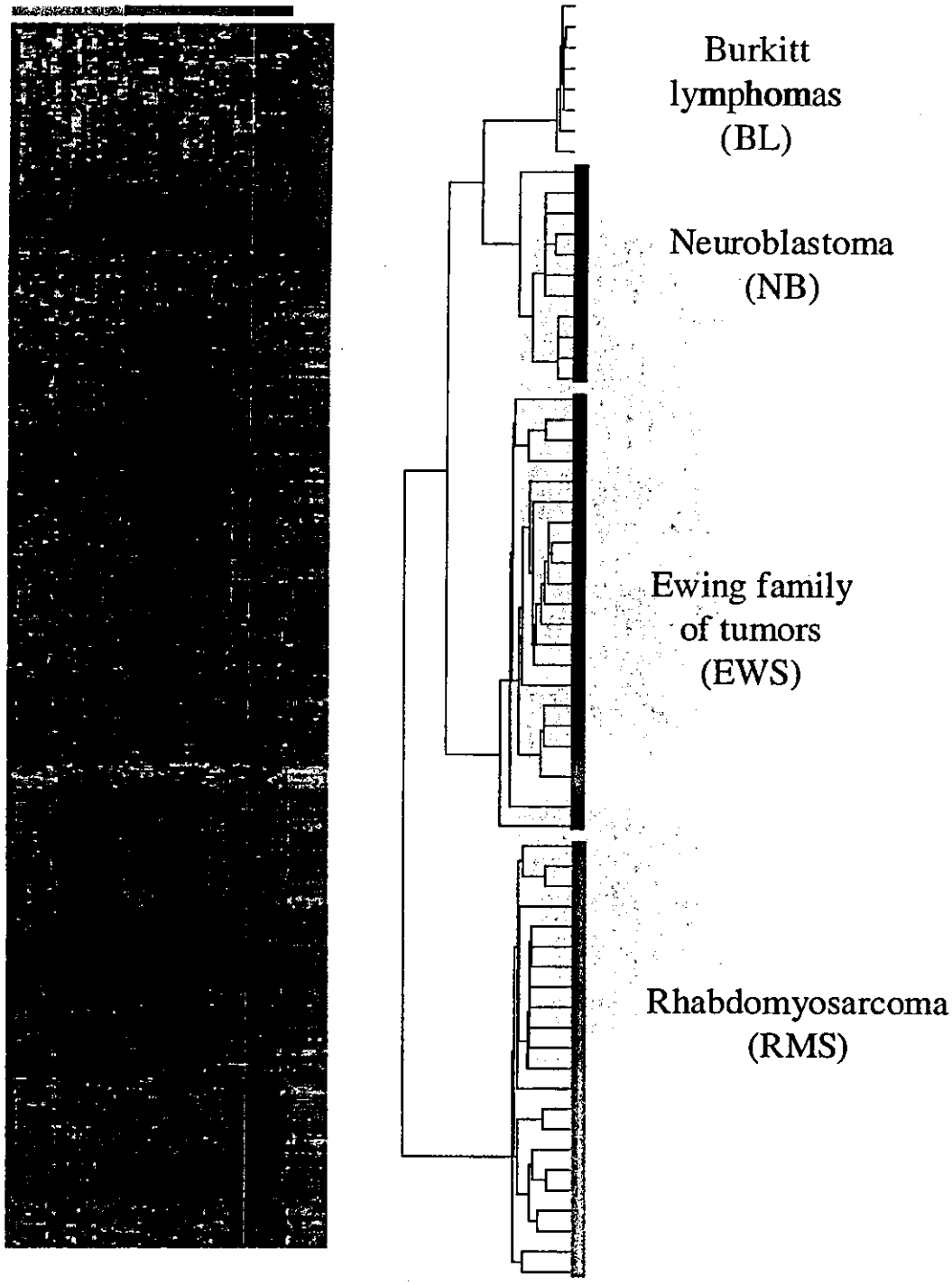

Figure 4: Predictor genes for to distinguish four subtypes of small, round blue cell tumors (SRBCTs), namely neuroblastoma (NB), rhabdomyosarcoma (RMS), non-Hodgkin lymphoma (NHL) and the Ewing family of tumors (EWS)[5]. A list of gene names is given in the supplementary information.

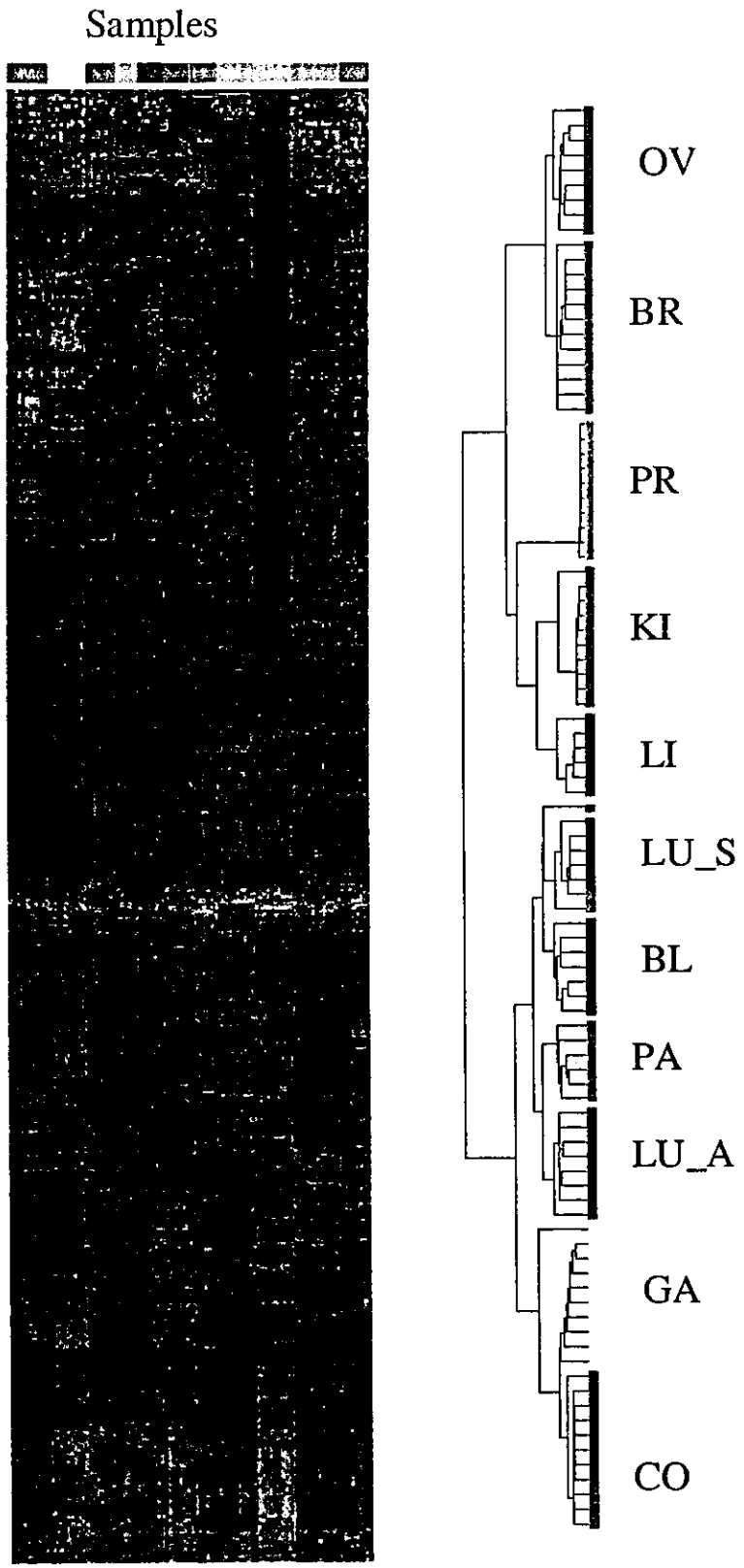

Figure 5: Predictor genes for the 11 tumor types in the dataset of [7]. The 11 tumor types are prostate (PR), breast(BR), lung (adenocarcinomas, LU_A, and squamous cell carcinomas, LU_S), ovary(OV), colorectum (CO), kidney(KI), liver(LI), pancreas(PA), bladder/ureter(BL) and gastroesophagus(GA). A list of gene names is given in the supplementary information.

Available online at www.sciencedirect.com
SCIENCE DIRECT
Gene 310 (2003) 17–28
GENE
AN INTERNATIONAL JOURNAL ON GENES AND GENOMES
www.elsevier.com/locate/gene

Characterization of the mouse *Abcc12* gene and its transcript encoding an ATP-binding cassette transporter, an orthologue of human ABCC12☆

Hidetada Shimizu[a], Hirokazu Taniguchi[b], Yoshitaka Hippo[b], Yoshihide Hayashizaki[c], Hiroyuki Aburatani[b], Toshihisa Ishikawa[a,*]

[a]*Department of Biomolecular Engineering, Graduate School of Bioscience and Biotechnology, Tokyo Institute of Technology, Nagatsuta 4259, Midori-ku, Yokohama 226-8501, Japan*
[b]*Genome Science Division, Research Center for Advanced Science and Technology, The University of Tokyo, 4-6-1 Komaba, Meguro-ku, Tokyo 153-8904, Japan*
[c]*Genome Exploration Research Group, Genome Science Laboratory, Genome Sciences Center, RIKEN, 1-7-22 Suehiro-cho, Tsurumi-ku, Yokohama 230-0045, Japan*

Received 13 December 2002; received in revised form 24 February 2003; accepted 6 March 2003
Received by T. Gojobori

Abstract

We have recently reported on two novel human ABC transporters, ABCC11 and ABCC12, the genes of which are tandemly located on human chromosome 16q12.1 [Biochem. Biophys. Res. Commun. 288 (2001) 933]. The present study addresses the cloning and characterization of Abcc12, a mouse orthologue of human ABCC12. The cloned Abcc12 cDNA was 4511 bp long, comprising a 4101 bp open reading frame. The deduced peptide consists of 1367 amino acids and exhibits high sequence identity (84.5%) with human ABCC12. The mouse *Abcc12* gene consists of at least 29 exons and is located on the mouse chromosome 8D3 locus where conserved linkage homologies have hitherto been identified with human chromosome 16q12.1. The mouse *Abcc12* gene was expressed at high levels exclusively in the seminiferous tubules in the testis. In addition to the Abcc12 transcript, two splicing variants encoding short peptides (775 and 687 amino acid residues) were detected. In spite of the genes coding for both ABCC11 and ABCC12 being tandemly located on human chromosome 16q12.1, no putative mouse orthologous gene corresponding to the human *ABCC11* was detected at the mouse chromosome 8D3 locus.

Keywords: ATP binding cassette transporter; Mouse; Abcc12; Mouse chromosome 8; Human chromosome 16; Sertoli cell

1. Introduction

The ATP-binding cassette (ABC) transporters form one of the largest protein families and play a biologically important role as membrane transporters or ion channel modulators (Higgins, 1992). According to the recently published draft sequence of the human genome, more than 50 human ABC transporter genes (including pseudogenes[1]) are anticipated to exist in the human genome. Hitherto 49 human ABC-transporter genes have been identified and sequenced (recent reviews: Klein et al., 1999; Dean et al., 2001; Borst and Oude Elferink, 2002). Based on the arrangement of their molecular structural components, i.e. the nucleotide binding domain and the topology of transmembrane spanning domains, human ABC transporters are classified into seven different gene families designated as A to G (the new nomenclature of human ABC transporter genes: http://gene.ucl.ac.uk/nomenclature/genefamily/abc.html). Mutations in the human ABC transporter genes have been reported to cause such genetic diseases as Tangier

☆ The cDNA sequences of mouse Abcc12 and its splice variants A and B have been registered in GenBank under the accession numbers of AF502146 (April 12, 2002), AF514414 (May 22, 2002), and AF514415 (May 22, 2002), respectively.

Abbreviations: ABC, ATP-binding cassette; EST, expresed sequence tag; MRP, multidrug resistance-associated protein; GAPDH, glutaraldehyde dehydrogenase; GS-X, pump, ATP-dependent glutathione *S*-conjugate export pump; RT–PCR, reverse transcriptase–polymerase chain reaction.

* Corresponding author. Tel.: +81-45-924-5800; fax: +81-45-924-5838.
E-mail address: tishikaw@bio.titech.ac.jp (T. Ishikawa).

[1] A truncated human ABC transporter, ABCC13 (GenBank accession number: AF418600), has most recently been cloned (Yabuuchi et al., 2002).

0378-1119/03/$ - see front matter © 2003 Elsevier Science B.V. All rights reserved.
doi:10.1016/S0378-1119(03)00504-3

disease, cystic fibrosis, Dubin–Johnson syndrome, Stargardt disease, and sitosterolemia (recent reviews: Dean et al., 2001; Borst and Oude Elferink, 2002).

We originally reported that transport of glutathione S-conjugates and leukotriene C_4 (LTC_4) across the cell membrane is mediated by an ATP-dependent transporter named the 'GS-X pump' (Ishikawa, 1989, 1992); however, the molecular nature of the transporter was not uncovered at that time. Later studies have provided evidence that the GS-X pump is encoded, at least, by the ABCC1 (MRP1) gene (Leier et al., 1994; Müller et al., 1994). ABCC1 (MRP1) was first identified by Cole et al. (1992) in the molecular cloning of cDNA from human multidrug-resistant lung cancer cells. After the discovery of the ABCC1 (MRP1) gene, six human homologues, ABCC2 (cMOAT/MRP2), ABCC3 (MRP3), ABCC4 (MRP4), ABCC5 (MRP5), ABCC6 (MRP6), and ABCC10 (MRP7) have been successively identified. Those ABC transporters exhibit a wide spectrum of biological functions and are involved in the transport of drugs as well as endogenous substances (see recent reviews: Borst and Oude Elferink, 2002; Ishikawa, in press).

Most recently, our group (Yabuuchi et al., 2001) and others (Tammur et al., 2001; Bera et al., 2001, 2002) have independently discovered two novel ABC transporters, human ABCC11 (MRP8) and ABCC12 (MRP9), that belong to the ABCC gene family. The predicted amino acid sequences of both gene products show a high similarity with ABCC5. The *ABCC11* and *ABCC12* genes consist of at least 30 and 29 exons, respectively, and they are tandemly located in a tail-to-head orientation on human chromosome 16q12.1 (Yabuuchi et al., 2001; Tammur et al., 2001). The physiological functions of these genes are not yet known; however recent linkage analyses have demonstrated that a putative gene responsible for paroxysmal kinesigenic choreoathetosis (PKC), a genetic disease of infancy, is located in the region of 16p11.2–q12.1 (Lee et al., 1998; Tomita et al., 1999). Since the *ABCC11* and *ABCC12* genes are encoded at that 16q12.1 locus, a potential link between the PKC gene and these ABC transporters has been implicated.

To elucidate the physiological function of human ABCC11 and ABCC12, knockout mice are considered to be a useful animal model. For this reason, we have undertaken the present study to pursue mouse orthologues of ABCC11 and ABCC12. In this study, we have cloned the cDNA of mouse Abcc12 and characterized its chromosomal location, gene organization, tissue-specific expression, the putative protein structure, and splicing variants.

2. Materials and methods

2.1. Cloning of mouse Abcc 12 cDNA

Mouse EST clones bearing a high similarity to partial sequences of human ABCC 12 cDNA were extracted from the NCBI mouse EST database and the mouse cDNA 'FANTOM 2' database of RIKEN (The FANTOM Consortium, 2002) by using the NCBI BLAST search program (Fig. 1). We have screened multiple tissue cDNA libraries (MTC, Clontech, Palo Alto, CA, USA) by PCR with the following primers deduced from the EST sequences: the forward primer, 5′-AGTTCCCTCATTTCAGCTCTCC-TAGGAC-3′, and the backward primer, 5′-GCAGGTA-GAGCTGACGATTAGCATAC-3′. High expression was detected in mouse testis.

To clone the mouse Abcc12 cDNA from the testis, we have designed four sets of PCR primers, as shown in Fig. 1. The PCR primer sets were as follows: c12-1 (the forward primer: 5′-GCCAAAAGTCGAGGGCTCCAAAACACC-3′ and the backward primer: 5′-GGCCACTGCTTTGACC-GAGAA-3′), c12-2 (the forward primer: 5′-GGCTGGC-TATGTCCAAAGTGGAA-3′ and the backward primer: 5′-GATGCCAAACATCAACACAGACACC-3′), c12-3 (the forward primer: 5′-GATGATGGGCAGCTCTGCTT-TC-3′ and the backward primer: 5′-TCACATGTCCA-TCGCCTCCTCTCA-3′), and c12-4 (the forward primer: 5′- GCCCGACTCTGCATTTGCGA-3′ and the backward primer: 5′-CAAAATCCAGGAACGCTGTCATCTCC-3′). The PCR reaction was performed with mouse testis cDNA (Clontech) and *Ex Taq* polymerase (TaKaRa, Japan), where the reaction consisted of 30 cycles of 95 °C for 30 s, 58 °C for 30 s, and 72 °C for 90 s. After agarose gel electrophoresis, the PCR products were extracted from the gels and subsequently inserted into TA cloning vectors (Invitrogen, Japan). The sequences of the inserts were analyzed with an automated DNA sequencer. (Toyobo Gene Analysis, Japan). The whole cDNA of mouse Abcc12 was obtained by assembling those partial sequences.

2.2. Detection of mouse Abcc 12 transcripts by PCR in different tissues

The expression of mouse Abcc 12 in different organs was examined by PCR with the mouse Multiple Tissue cDNA (MTC, Clontech). Two sets of PCR primers were designed to detect the corresponding transcript (Fig. 1), namely, the primer set #1 detecting the 5′-part of Abcc12 cDNA (the forward primer: 5′-CCACTGTCTCCTTATGACTCATCG-GAC-3′, the backward primer: 5′-GGGACAAAACAAGG-CAGCCTCAAAC-3′) and the primer set #2 recognizing the 3′-part of Abcc12 cDNA (the forward primer: 5′-TAT-GGCCCGGGCACTTCTCCGTAA-3′, the backward primer 5′-GACCTTTACAGTCCAACCTCTGCAGCTAGT-3′). The PCR reaction consisted of 35 cycles of 95 °C for 30 s, 58 °C for 30 s, and 72 °C for 30 s. The reaction products were detected by agarose gel electrophoresis.

2.3. Northern blot analysis

Mouse organs (i.e. heart, kidney, brain, testis, spleen, stomach, liver, thymus, and small intestine) were surgically

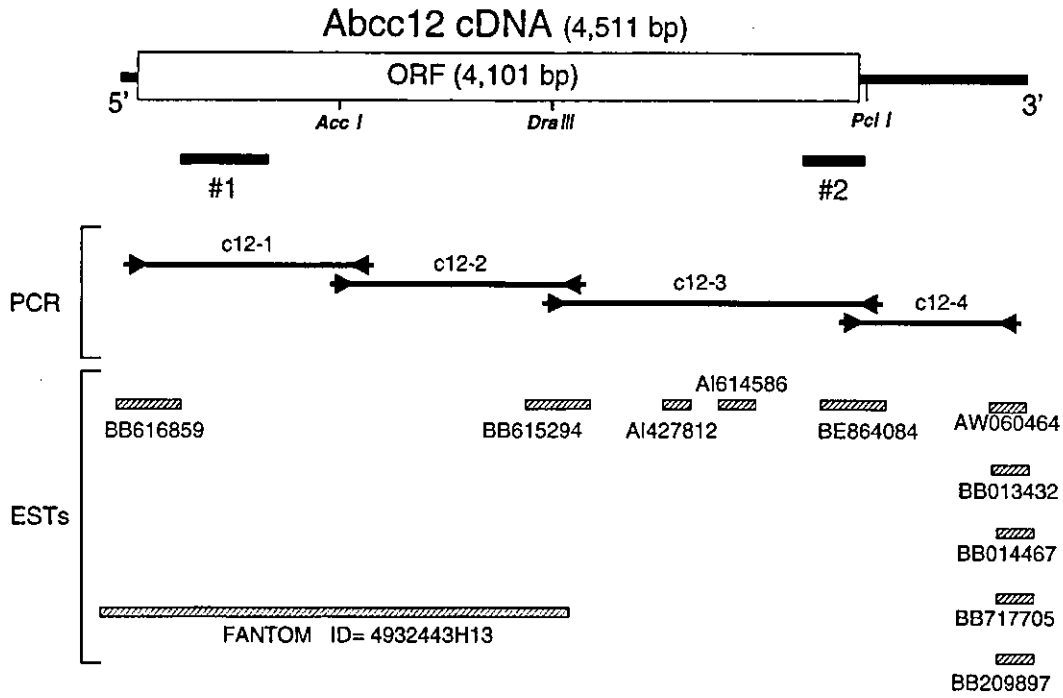

Fig. 1. Strategy for the cloning of mouse Abcc12 cDNA. The open reading frame (ORF) is indicated by a box. The cleavage sites by restriction enzymes (*Acc*I, *Dra*III and *Pci*I) are also indicated. The cDNA was cloned by PCR with four sets of primers, c12-1, c12-2, c12-3, and c12-4, as described in Section 2. The forward and backward PCR primers are indicated by arrows, and the resulting PCR products are represented by straight lines. ESTs and the FANTOM 2 cDNA are sorted according to the sequence homology with Abcc12 cDNA. PCR products used to detect the Abcc12 transcript in different tissues are indicated by #1 and #2.

excised from Balb/C mice (10 weeks old) under anesthesia and immediately frozen in liquid nitrogen. The tissue was pulverized in a mortar containing liquid nitrogen. The resulting tissue powder was subsequently homogenized in TRIzol (Invitrogen, Japan) by using a Polytron homogenizer, and total RNA was extracted according to the manufacturer's protocol. A sample (15 μg/lane as determined by absorbance at 260 nm) of RNA, thus prepared, was subjected to electrophoresis in 1% (w/v) agarose gels containing formaldehyde and then transferred to Hybond-XL membranes (Amersham Pharmacia Biotech). RNA was fixed on the membrane surface by baking at 80 °C for 2 h.

Three different DNA probes encoding partial sequences (463–1165; 1440–2116; 3660–4154) of the Abcc12 cDNA ORF were prepared and separately labeled with [^{32}P]dCTP by using the BcaBest labeling kit (TaKaRa) according to the random-primed labeling method. Hybridization with those DNA probes was carried out according to the hybridization protocol of the Expresshybri kit (Clontech), and the hybridization signal was detected in a BASS 2000 (Fuji Film, Japan).

2.4. Laser-captured microdissection and RT–PCR

The frozen tissue of mouse testis was cut into thin sections (5 μm thickness) with a microtome (Leika GmbH, Germany) and mounted onto glass slides. The tissue slice on the glass slide was stained in 70% Giemsa solution. After staining, the tissue slices were dehydrated in 100% ethanol and subsequently in 100% xylene. The slide was air-dried, and the seminiferous tubules and the interstitium in the tissue slices were excised by laser-capture microdissection with an Arcturus PixCell 2 LCM system (Arcturus Engineering, Mountain View, CA). The dissected samples were homogenized in 200 μl of TRIzol, and RNA was extracted. mRNA was then converted to cDNA by reverse transcriptase (RT) using a SensiScripts kit (Qiagen). Expression of mouse Abcc12 in these samples was detected by PCR with the same primers and under the same conditions as described in Section 2.2.

2.5. In situ hybridization

The testis was surgically excised from mice under anesthesia and immersed in phosphate-buffered saline (PBS) containing 4% paraformaldehyde. The tissue was embedded in paraffin, and thin sections (4 μm thickness) were prepared with a microtome. The resulting thin sections were soaked in xylene three times (3 min for each) and twice in 100% ethanol (3 min for each). Thereafter, sections were rinsed in 70% ethanol and subsequently in 0.1% DEPC-treated water three times. Prior to hybridization, the sections were treated with proteinase K (1:400 v/v) in Tris-buffered saline (TBS) at room temperature for 10 min and

A

```
Mouse Abcc12    1 MVGEGPYLISDLDRRGHRRSFAERYDPSLKTMIPVRPRARLAPNPVDDAGLLSFATFSWL 60
Human ABCC12    1 MVGEGPYLISDLDQRGRRRSFAERYDPSLKTMIPVRPCARLAPNPVDDAGLLSFATFSWL 60

Mouse Abcc12   61 TPVMIRSYKHTLTVDTLPPLSPYDSSDINAKRFQILWEEEIKRVGPEKASLGRVVWKFQR 120
Human ABCC12   61 TPVMVKGYRQRLTVDTLPPLSTYDSSDTNAKRFRVLWDEEVARVGPEKASLSHVVWKFQR 120

Mouse Abcc12  121 TRVLMDVVANILCIVMAALGPTVLIHQILQHITSISSGHIGIGICLCLALFTTEFTKVLF 180
Human ABCC12  121 TRVLMDIVANILCIIMAAIGPTVLIHQILQQTERTSG-KVWVGIGLCIALFATEFTKVFF 179

Mouse Abcc12  181 WALAWAINYRTAIRLKVALSTLIFENLLSFKTLTHISAGEVLNILSSDSYSLFEAALFCP 240
Human ABCC12  180 WALAWAINYRTAIRLKVALSTLVFENLVSFKTLTHISVGEVLNILSSDSYSLFEAALFCP 239

Mouse Abcc12  421 PPSYITQPEDPDTILLLANATLTWEQEINRKSDPPKAQIQKRHVFKKQRPELYSEQSRSD 480
Human ABCC12  420 PPSYITQPEDPDTVLLLANATLTWEHEARQESTPKKLQNQKRHLCKKQRSEAYSERSPPA 479
                                                  Walker A
Mouse Abcc12  481 QGVASPEWQSGSPKSVLHNISFVVRKGKVLGICGNVGSGKSSLISALLGQMQLQKGVVAV 540
Human ABCC12  480 KGATGPEEQSDSLKSVLHSISFVVRKGKILGICGNVGSGKSSLLAALLGQMQLQKGVVAV 539

Mouse Abcc12  541 NGPLAYVSQQAWIFHGNVRENILFGEKYNHQRYQHTVHVCGLQKDLNSLPYGDLTEIGER 600
Human ABCC12  540 NGTLAYVSQQAWIFHGNVRENILFGEKYDHQRYQHTVRVCGLQKDLSNLPYGDLTEIGER 599
                        Signature C      Walker B
Mouse Abcc12  601 GVNLSGGQRQRISLARAVYANRQLYLLDDPLSAVDAHVGKHVFEECIKKTLKGKTVVLVT 660
Human ABCC12  600 GLNLSGGQRQRISLARAVYSDRQLYLLDDPLSAVDAHVGKHVFEECIKKTLRGKTVVLVT 659

Mouse Abcc12  661 HQLQFLESCDEVILLEDGEICEKGTHKELMEERGRYAKLIHNLRGLQFKDPEHIYNVAMV 720
Human ABCC12  660 HQLQFLESCDEVILLEDGEICEKGTHKELMEERGRYAKLIHNLRGLQFKDPEHLYNAAMV 719

Mouse Abcc12  721 ETLKESPAQRDEDAVLASGDEKDEGKEPETEE-FVDTNAPAHQLIQTESPQEGIVTWKTY 779
Human ABCC12  720 EAFKESPAEREEDAVLAPGNEKDEGKESETGSEFVDTKVPEHQLIQTESPQEGTVTWKTY 779

Mouse Abcc12  780 HTYIKASGGYLVSFLVLCLFFLMMGSSAFSTWWLGIWLDRGSQVVCASQNNKTACNVDQT 839
Human ABCC12  780 HTYIKASGGYLLSLFTVFLFLLMIGSAAFSNWWLGLWLDKGSRMTCGPQGNRTMCEVGAV 839

Mouse Abcc12  840 LQDTKHHMYQLVYIASMVSVLMFGIIKGFTFTNTTLMASSSLHNRVFNKIVRSPMSFFDT 899
Human ABCC12  840 LADIGQHVYQRVYTASMVFMLVFGVTKGFVFTKTTLMASSSLHDTVFDKILKSPMSFFDT 899

Mouse Abcc12  900 TPTGRLMNRFSKDMDELDVRLPFHAENFLQQFFMVVFILVIMAAVFPVVLVVLAGLAVIF 959
Human ABCC12  900 TPTGRLMNRFSKDMDELDVRLPFHAENFLQQFFMVVFILVILAAVFPAVLLVVASLAVGF 959

Mouse Abcc12  960 LILLRIFHRGVQELKQVENISRSPWFSHITSSIQGLGVIHAYDKKDDCISKFKTLNDENS 1019
Human ABCC12  960 FILLRIFHRGVQELKKVENVSRSPWFTHITSSMQGLGIIHAYGKKESCIT-Y-------- 1010

Mouse Abcc12 1020 SHLLYFNCALRWFALRMDILMNIVTFVVALLVTLSFSSISASSKGLSLSYIIQLSGLLQV 1079
Human ABCC12 1011 -HLLYFNCALRWFALRMDVLMNILTFTVALLVTLSFSSISTSSKGLSLSYIIQLSGLLQV 1069

Mouse Abcc12 1080 CVRTGTETQAKFTSAELLREYILTCVPEHTHPFKVGTCPKDWPSRGEITFKDYRMRYRDN 1139
Human ABCC12 1070 CVRTGTETQAKFTSVELLREYISTCVPECTHPLKVGTCPKDWPSCGEITFRDYQMRYRDN 1129
                                  Walker A
Mouse Abcc12 1140 TPLVLDGLNLNIQSGQTVGIVGRTGSGKSSLGMALFRLVEPASGTIIIDEVDICTVGLED 1199
Human ABCC12 1130 TPLVLDSLNLNIQSGQTVGIVGRTGSGKSSLGMALFRLVEPASGTIFIDEVDICILSLED 1189

Mouse Abcc12 1200 LRTKLTMIPQDPVLFVGTVRYNLDPLGSHTDEMLWHVLERTFMRDTIMKLPEKLQAEVTE 1259
Human ABCC12 1190 LRTKLTVIPQDPVLFVGTVRYNLDPFESHTDEMLWQVLERTFMRDTTMKLPEKLQAEVTE 1249
                        Signature C      Walker B
Mouse Abcc12 1260 NGENFSVGERQLLCMARALLRNSKIILLDEATASMDSKTDTLVQSTIKEAFKSCTVLTIA 1319
Human ABCC12 1250 NGENFSVGERQLLCVARAILRNSKIILLDEATASMDSKTDTLVQNTIKDAFKGCTVLTIA 1309

Mouse Abcc12 1320 HRLNTVLNCDLVLVMENGKVIEFDKPEVLAEKPDSAFAMLLAAEVGL 1366
Human ABCC12 1310 HRLNTVLNCDHVLVMENGKVIEFDKPEVLAEKPDSAFAMLLAAEVRL 1356
```

Fig. 2. Alignments of the mouse Abcc12 and human ABCC12 proteins. (A) Amino acid sequences were aligned by using the GENETYX-MAC program. The Walker A and B motifs as well as the signature C are indicated by boxes. (B) The hydropathy plots of mouse Abcc12 (this study) and human ABCC12 (Yabuuchi et al., 2001). The hydropathy profiles were calculated according to the Kyte and Doolittle (1982) algorithm.

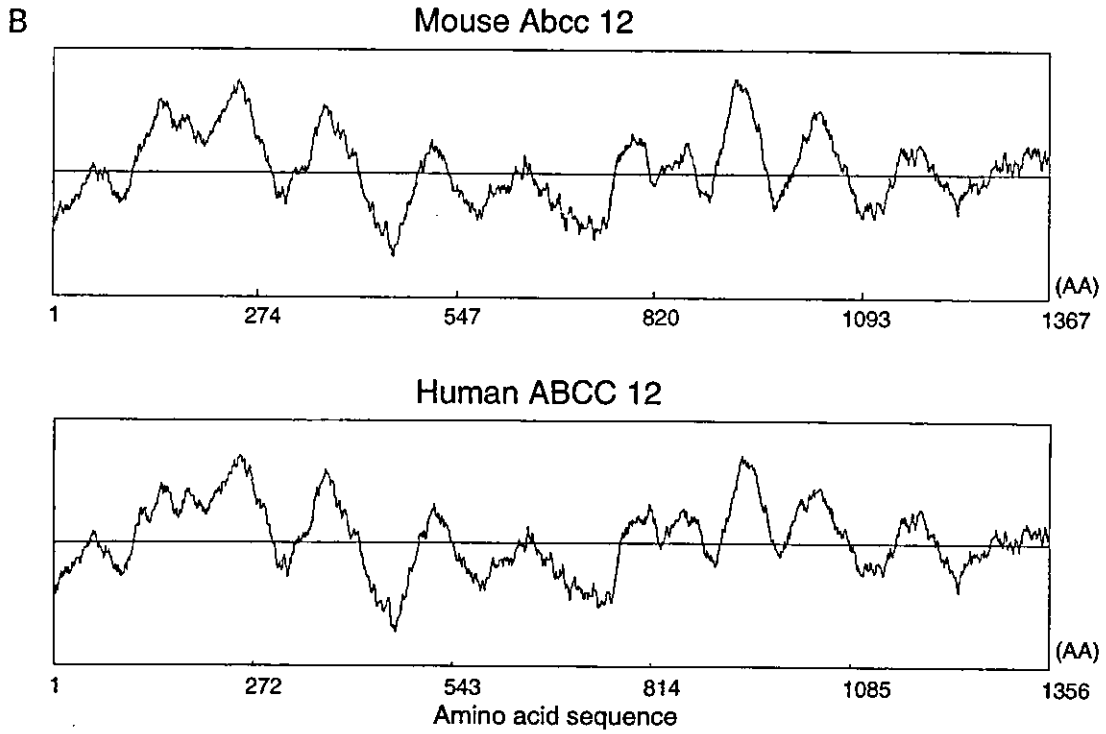

Fig. 2 (*continued*)

then rinsed with 0.1% DEPC-treated water. The following biotin-labeled oligonucleotide DNA probes were synthesized, i.e. the sense probe: 5′-AGCCTGACTCTGCATTTGCGATGTTACTAGCTGCAG-3′ and the anti-sense probe: 5′-CTGCAGCTAGTAACATCGCAAATGCAGAGTCAGGCT-3′. The probes were diluted in the DAKO in situ hybridization solution (DAKO S3304) at a final concentration of 1 ng/ml. The hybridization with the sense or the anti-sense probe was carried out on the thin section at 37 °C overnight. Thereafter, the slides were incubated in 0.1× SSC (300 mM sodium chloride and 1.5 mM sodium citrate, pH 7.0) at 37 °C for 20 min twice and washed in TBS at room temperature for 3 min.

In situ hybridization signals were visualized by a tyramide amplification signal detection system using the DAKO GenPoint system (DAKO K0620), according to manufacturer's instructions. Finally, the sections were counterstained with Mayer's hematoxylin (Sigma, USA).

2.6. Data analysis

DNA sequences were analyzed with the GENETYX-MAC software ver.11 and compared with other ABCC transporter genes registered in the NCBI database. The hydropathy profile of the protein deduced from the cDNA sequence was calculated with the Kyte and Doolittle hydropathy algorithm (Kyte and Doolittle, 1982), and the SOSUI program (http://sosui.proteome.bio.tuat.ac.jp/sosuimenu0.html) was used to predict transmembrane domains. Phylogenic relationships were calculated by using the distance-based neighbor-joining method (Saitou and Nei, 1987).

3. Results

3.1. Cloning and characterization of mouse Abcc 12 cDNA

Fig. 1 depicts the strategy of cloning mouse Abcc12 cDNA. The sequence of human ABCC12 cDNA was applied to the currently available mouse EST database on an NCBI BLAST search to discover ESTs encoding partial sequences of mouse Abcc 12. Thereby, the following EST clones were extracted: BB616859, BB615294, AI427812, AI614586, BE864084, AW060464, BB013432, BB014467, BB717705, and BB209897. In addition, in a search of the FANTOM 2 database of RIKEN, we found one cDNA clone (ID number = 4932443H13) that exhibited a high sequence homology with human ABCC12 cDNA. Based on those ESTs as well the partial cDNA clone (ID = 4932443H13), we designed four sets of PCR primers to clone the mouse Abcc12 cDNA (see Section 2 for experimental details). By PCR, we obtained a total of four cDNA fragments (Fig. 1) and assembled them to construct the full cDNA encoding mouse Abcc12.

Table 1
Amino acid sequence identity of the mouse Abcc 12 with human ABC proteins in the ABCC sub-family

ABC protein	Identity (%)
ABCC1	33.4
ABCC2	32.1
ABCC3	31.1
ABCC4	40.2
ABCC5	43.7
ABCC6	28.5
CFTR (ABCC7)	27.9
ABCC8	30.6
ABCC9	27.9
ABCC10	34.6
ABCC11	47.8
ABCC12	84.5

The amino acid sequences of human ABC proteins were acquired from the NCBI database (refer to the accession numbers given in the legend of Fig. 3).

3.2. Characterization of mouse Abcc12 cDNA in comparison with members of the human ABCC sub-family

The cloned mouse Abcc12 cDNA (GenBank accession number: AF502146) was 4511 bp long, containing a 4101 bp open reading frame (ORF). The Abcc12 cDNA has a Kozak consensus initiation sequence (Kozak, 1991) for translation around the first ATG region, namely, 5′-ATCAAGATGG-3′. The amino acid sequence deduced from the cDNA sequence with the GENETYX-MAC program revealed that the cDNA encodes a single peptide consisting of 1366 amino acid residues (Fig. 2A). Motif analysis predicted the existence of two sets of ATP-binding cassettes (Walker et al., 1982): namely, Walker A (amino acids 514–521 and 1161–1168), Walker B (amino acids 624–628 and 1284–1288), and signature C motifs (amino acids 604–618 and 1264–1278) (Fig. 2A). Fig. 2B shows the hydropathy plots of mouse Abcc12 and human ABCC12, demonstrating a remarkable similarity between these transporters.

Table 1 shows that the amino acid sequence of mouse Abcc12 has the highest identity with human ABCC12 among the hitherto known members of the human ABCC sub-family. The sequence identity of mouse Abcc12 with human ABCC12 was 84.5%, whereas its identity with human ABCC11 was 47.8%. The identity of mouse Abcc12 with other human members was relatively low, in the range of 27.9 to 43.7% (Table 1).

Fig. 3 shows the phylogenic relationship among the members of the human and mouse ABCC subfamily. Mouse Abcc12, as well as human ABCC12, apparently belongs to a cluster named 'Class D' that comprises ABCC4, ABCC5, ABCC11, Abcc4, and Abcc5 (see Section 4 for the classification).

3.3. Chromosomal location of the mouse Abcc 12 gene

Fig. 4 shows the location of the *Abcc12* gene on the mouse chromosome 8. The mouse Abcc12 gene spans a 65 kb length and is located between two microsatellite markers, D8Mit347 and D8Mit348, at the D3 region of the mouse chromosome 8 (Fig. 4), as referred to in the mouse genome databases of NCBI and EMBL/UCSC (Mouse Genome Sequencing Consortium, 2002). This genome region of the mouse chromosome 8 is reportedly related to human chromosome 16q12.1, where the human *ABCC11* and *ABCC12* genes are tandemly located (Yabuuchi et al., 2001; Tammur et al., 2001). Comparison of the cloned

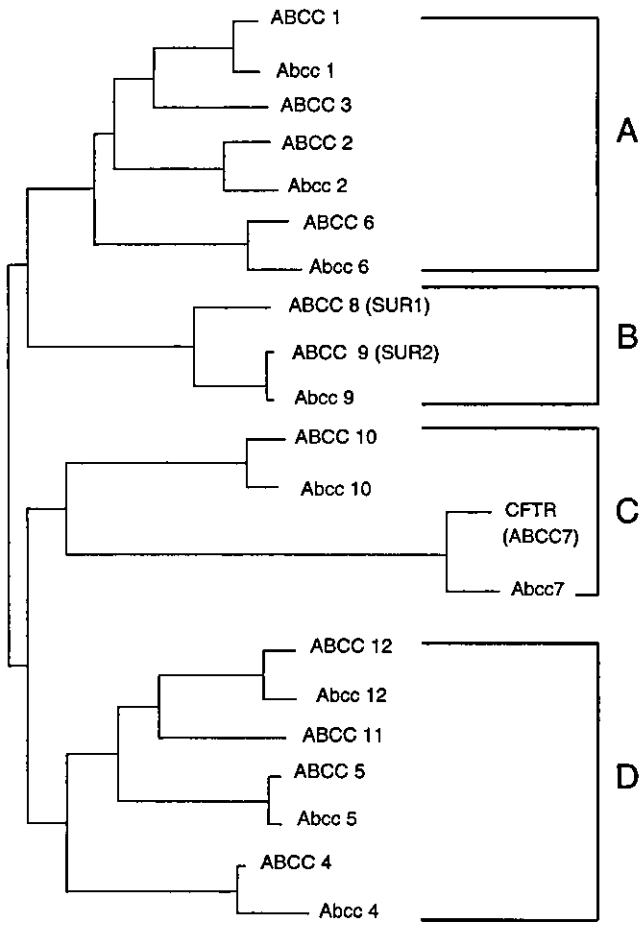

Fig. 3. The phylogenetic relationship among hitherto characterized members of the human and mouse ABCC sub-family. The phylogenetic distance was calculated according to the distance-based neighbor-joining method (Saitou and Nei, 1987). For the sequences of those ABC transporters, accession numbers are as follows: human ABCC1 (NM004996), ABCC2 (NM000392), ABCC3 (Y17151), ABCC4 (NM005845), ABCC5 (NM005688), ABCC6 (NM001171), ABCC7 (NM000492), ABCC8 (NM000352), ABCC9 (NM005691), ABCC10 (AK000002), ABCC11 (AF367202), ABCC12 (NM033226) mouse Abcc1 (NM008576), Abcc2 (NM013806), Abcc4 (D630049P08), Abcc5 (NM013790), Abcc6 (NM018795), Abcc7 (NM021050), Abcc8 (XM133448), Abcc9 (NM011511), Abcc10 (AF406642), Abcc12 (AF502146).

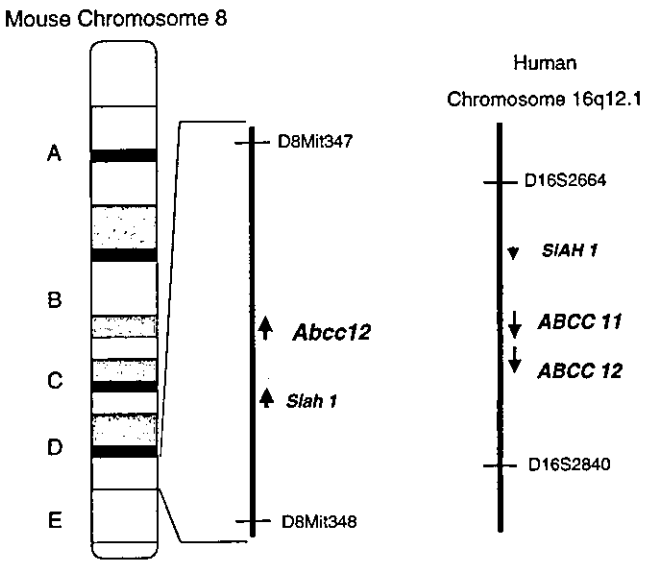

Fig. 4. Location of the *Abcc12* gene on mouse chromosome 8. *Abcc12* and *Siah 1* genes are located in the mouse chromosomal region between two microsatellite markers, D8Mit347 and D8Mit348. Human *ABCC11*, *ABCC12*, and *SIAH 1* genes are located in the region between D16S2664 and D16S2840 on the human chromosome 16q12.1.

Abcc12 cDNA with the mouse genome data revealed that the *Abcc12* gene consists of at least 29 exons, where the translation start codon (ATG) was found in exon 1. In addition, two sets of ATP-binding cassettes were detected. The first Walker A motif is located in the exon 10, whereas the second Walker A motif spreads over exons 24 and 25. Two Walker B motifs are encoded in exons 13 and 28, and two signature C motifs are located in exons 13 and 27.

Table 2 summarizes the exon and intron boundaries with partial sequences at each splicing site of the *Abcc12* gene; however, the partial sequences of the introns proximal to both 5′- and 3′-ends of exon 3 are presently not available (Table 2). These results suggest that the splicings of the mouse Abcc12 gene follow the conventional GT–AG rule, except for the exon 19.

3.4. Tissue-dependent expression of the mouse Abcc 12 gene

Fig. 5A shows the expression levels of the mouse Abcc12 gene in different organs as detected by RT–PCR with two different sets of PCR primers #1 and #2 (see Fig. 1 and Section 2 for details). The products of PCR reactions with primers #1 and #2 were 486 and 288 bp, respectively. Among the organs tested, the highest expression (mRNA) of

Table 2
Partial sequences of intron/exon and exon/intron boundaries in the mouse *Abcc 12* gene

Exon	Size (bp)	Intron/Exon		Exon/Intron	
1	152	tgtcccgaag	CCAAGAGTCG	CCCGTGCAAG	gtgagccagg
2	156	tttgctctag	GTTGGCACCC	ACGCCAAGAG	gtaccaggct
3[a]	147	nnnnnnnn	ATTCCAGATC	CTTGGGGCCG	nnnnnnnn
4	238	tgttttacag	ACAGTTCTCA	TGCAGGCGAG	gtaagcaggg
5	174	ttctttctag	GTACTCAATA	CCCGATCCAG	gtaagttggg
6	148	tcgatttcag	ATGTTTATGG	ACCATTCACG	gtaagatgag
7	149	tcttttgcag	ACATAAGAAA	TGCCCCTGTG	gtaagagtta
8	108	cctccttcag	GCATTTAGTG	GAGAATGAAG	gtataagtaa
9	279	ttaatctcag	AAAATCCTCA	GGTGAGAAAG	gtgagtgtat
10	72	tctctgacag	GGGAAGGTCT	CCTAGGACAG	gtgagtgtgt
11	125	atcgctctag	ATGCAGTTAC	ACCACCAAAG	gtattattaa
12	73	atgtctacag	GTACCAACAC	CCTGACTGAG	gtaagcagag
13	204	ctgtccacag	ATTGGAGAGC	CCAGTTGCAG	gtgactggga
14	135	gtctctgcag	TTCCTGGAGT	GCAATTCAAG	gtaaactgca
15	76	ttatctccag	GATCCAGAGC	GAAGACGCTG	gtacagtcag
16	69	ctcatcctag	TCTTGGCTTC	GACACAAACG	gtatttacca
17	90	gtctctgcag	CTCCCGCTCA	GCTTCTGGAG	gtttagtata
18	104	tctccggcag	GGTACCTGGT	GGGTTCCCAG	gtgagtttcc
19	194	tgtgttgcag	GTCGTCTGTG	GAGTATTTAATA	caaggtagaa
20	229	ttctaccctc	AGATCGTCAG	TTCTTTTACG	gtaggattat
21	138	tcccccacag	CATCTTCCAT	GCATCAGCAA	gtgagtggat
22	187	ttgactttag	GTTTAAGACA	CATCATCCAG	gtaacggctg
23	90	ttcccaacag	CTCAGTGGAT	GTACATTTTG	gtaaggaatg
24	190	tgcttttcag	ACCTGTGTTC	ACGGGCTCCG	gtgaggacag
25	160	ttgtccccag	GAAAATCATC	GTACAGTAAG	gtagctgttt
26	79	ttcgttgcag	GTACAACTTG	GAGAGACACA	gtacgtcttg
27	114	tgttttatag	ATAATGAAAC	TAATTCAAAA	gtaaggaaac
28	165	tccttaacag	ATCATTCTCC	AAATGGGAAG	gtgcaggaaa
29	464	tgattttcag	GTGATTGAGT	CCTGGATTTT	gttaccagac

[a] The partial sequences of the introns proximal to the 5′- and 3′-ends of exon 3 are not available, therefore they are represented by 'nnnn'.

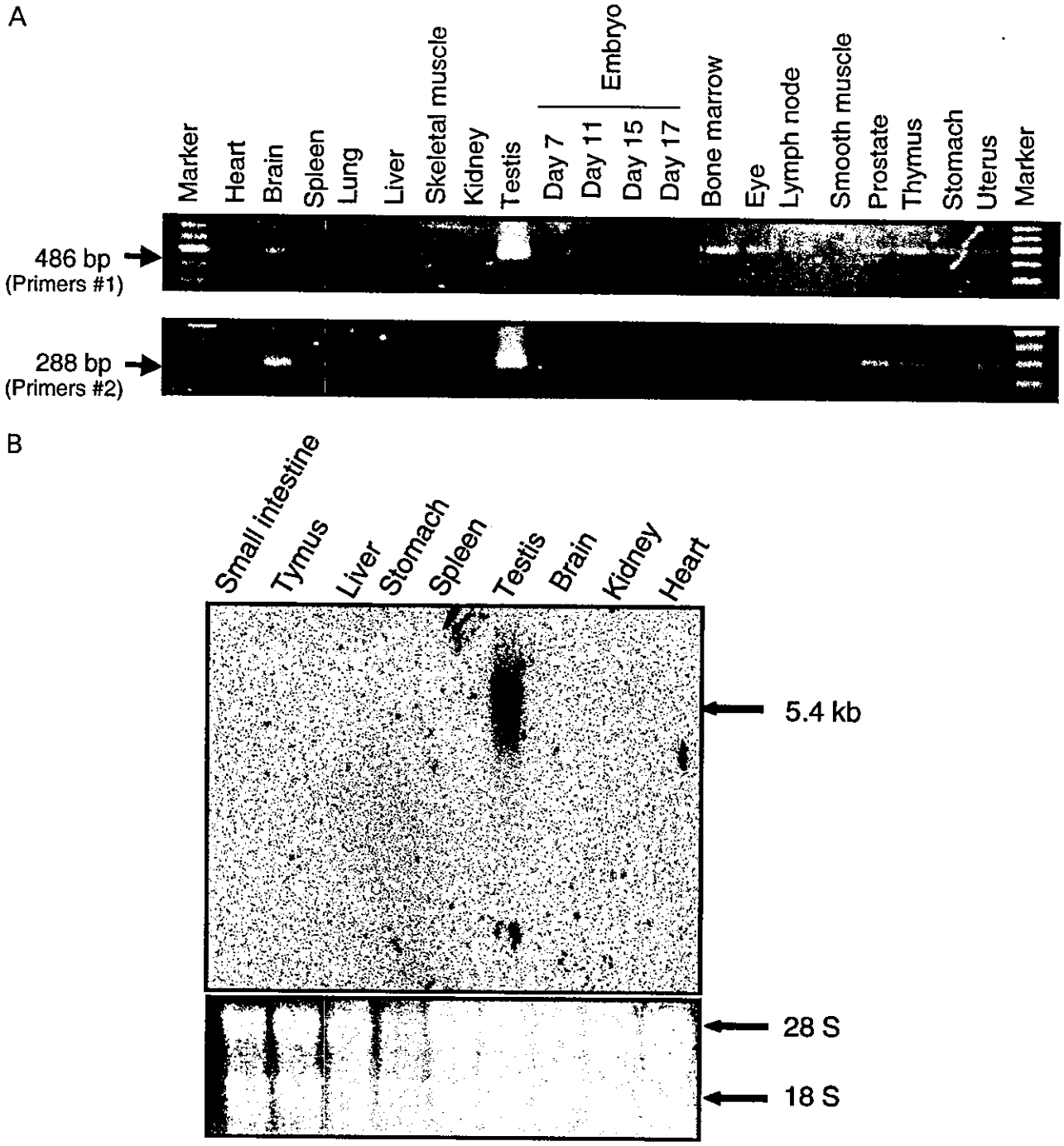

Fig. 5. Expression of the mouse *Abcc12* gene in different tissues. The Abcc12 transcript was detected by PCR (A) and by Northern hybridization (B) as described in Section 2. For the PCR detection (A), two sets of primers (#1 and #2; Fig. 1) were used. The resulting PCR products were 486 and 288 bp, as indicated by arrows. For the Northern hybridization (B), RNA (15 μg/lane) prepared from mouse tissues was fractionated by electrophoresis in 1.0% (w/v) agarose gels and visualized by ethidium bromide (bottom). 18S and 28S rRNAs are indicated by arrows. Northern hybridization (top) with a ^{32}P-labeled probe was carried out as described in Section 2. The detected Abcc12 mRNA (5.4 kb) is indicated by an arrow.

Abcc12 was observed in the testis. Relatively lower expression was detected in the brain, bone marrow, eye, lymph node, prostate, thymus, stomach, and uterus in the adult mouse. Northern blot hybridization (Fig. 5B) clearly demonstrates the predominant expression of mouse Abcc12 in the testis, being consistent with the results of RT–PCR (Fig. 5A). The transcript size of mouse Abcc 12 was about 5.4 kb.

3.5. Localization of mouse Abcc 12 in the testis

To elucidate the expression site of Abcc12 in the mouse testis, we have carried out laser-captured microdissection and RT–PCR. The seminiferous tubules and the interstitium were dissected, and RNA was extracted to prepare cDNA (see Section 2). PCR was carried out with the same primer

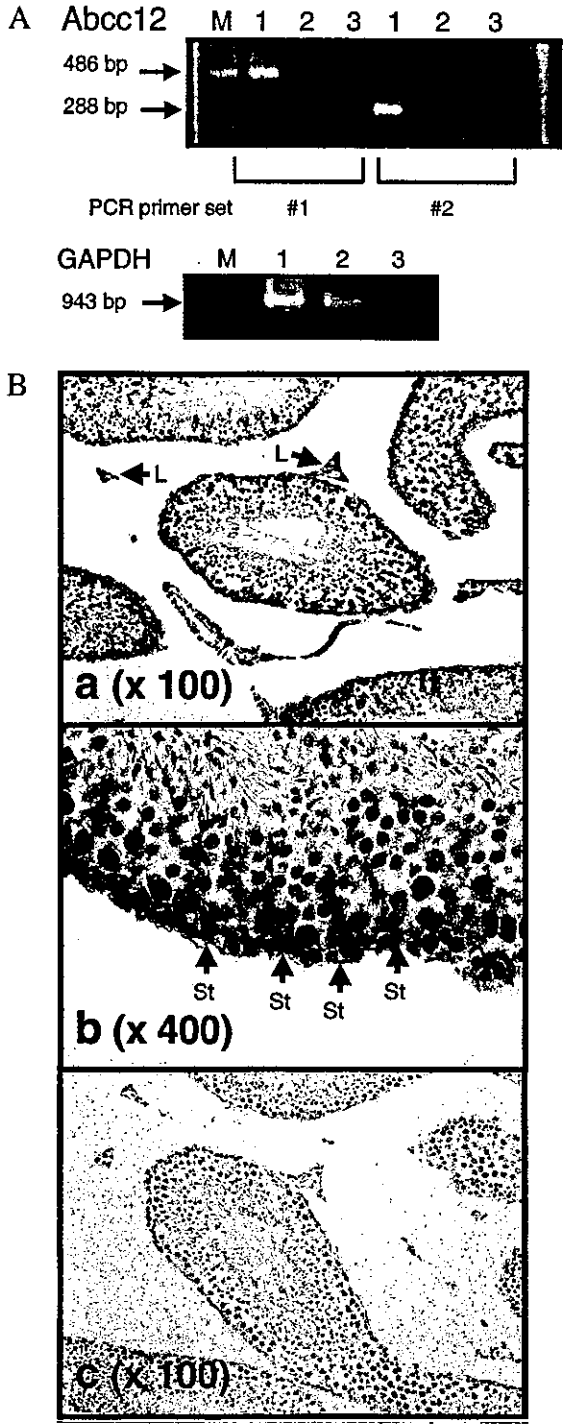

Fig. 6. Detection of the Abcc12 transcript in the mouse testis by means of laser-captured microdissection and RT–PCR (A) as well as by in situ hybridization (B). (A) Abcc12 and GAPDH transcripts were detected by PCR with RT reaction products prepared from micro-dissected samples. For the PCR detection, two sets of primers (#1 and #2; Fig. 1) were used, and the resulting PCR products were 486 and 288 bp, as indicated by arrows. The 943 bp product of GAPDH is the positive control for the PCR reaction. Lane M, DNA size markers; lane 1, seminiferous tubules; lane 2, stroma cells; lane 3, without RT reaction products. (B) The Abcc12 transcript in the mouse testis was detected by in situ hybridization as described in Section 2. Panels a and b show the results of hybridization with the anti-sense probe, whereas panel c shows the negative control, i.e. hybridization with the sense probe. Magnifications are indicated in parentheses. Arrows indicate Leydig (L) and Sertoli (St) cells.

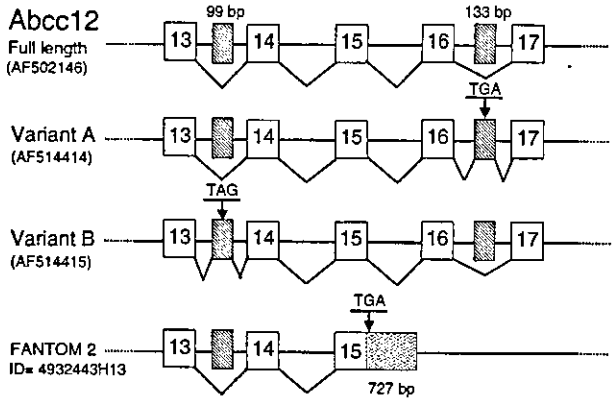

Fig. 7. Schematic illustration for alternative splicing of the *Abcc12* gene. Exons are numbered according to the sequence of the cloned Abcc12 cDNA. Variant A cDNA has one extra exon (133 bp) with a stop codon (TGA) between exons 16 and 17. Variant B cDNA has one extra exon (99 bp) with a stop codon (TAG) between exons 13 and 14. The exon 15 of the FANTOM 2 cDNA (ID = 4932443H13) has a 727 bp extension, as compared with the exon 15 of Abcc12 cDNA.

sets #1 and #2 as described above. As shown in Fig. 6A, Abcc12 expression was exclusively high in the seminiferous tubules, whereas little expression was detected in the interstitium. To gain further insight into cell type-specific expression of the *Abcc12* gene, we carried out in situ hybridization. Fig. 6B depicts the results of the in situ hybridization, demonstrating that the expression of Abcc12 was high in Sertoli cells of the seminiferous tubules (Fig. 6B, panel b). In addition, expression of Abcc12 was also detected in Leydig cells of the interstitium (Fig. 6B, panel a) under our hybridization conditions. No hybridization signal was observed with the sense probe, as the negative control (Fig. 6B, panel c).

3.6. Splicing variants of *Abcc12*

During the cloning of Abcc12 cDNA in the present study, we have discovered two variant forms of Abcc12 (GenBank accession numbers: AF514414 and AF514415 for variants A and B, respectively). Fig. 7 summarizes the configurations of those variants of the Abcc12 transcript together with the partial cDNA (ID = 4932443H13) reported in the FANTOM 2 database. The cDNAs of both variants A and B consist of 30 exons. As shown in Fig. 7, the variant A cDNA has an extra exon (133 bp) located between exons 16 and 17. Although the variant A cDNA consists of a total of 30 exons, the variant A is considered to encode a short peptide (775 amino acid residues), because the extra exon has a translation stop codon, TGA (Fig. 7). Likewise, the variant B cDNA has one extra exon (99 bp) with a stop codon (TAG) between exons 13 and 14 (Fig. 7), and, therefore, it also encodes a short peptide (687 amino acid residues). On the other hand, the FANTOM 2 cDNA (ID = 4932443H13) cloned by the 5′-oligo-cap method (Carninci et al., 1996) has an extension (121 bp) at the

5′-end of the cDNA, as compared with the cloned Abcc12 cDNA (data not shown). It is noteworthy that the exon 15 of the FANTOM 2 cDNA is different from that of the Abcc12 cDNA cloned in this study, although the other exons 2–14 are identical. Indeed, the exon 15 in the FANTOM 2 cDNA is 727 bp larger than the exon 15 of Abcc12 cDNA, but it encodes a translation stop codon (TGA) in the extended sequence (Fig. 7).

4. Discussion

4.1. Molecular characteristics of mouse Abcc12 cDNA

In the present study, we have cloned and characterized the cDNA of a new mouse ABC transporter, named Abcc12. The cloned cDNA was 4511 bp long and comprised a 4101 bp open reading frame. The deduced peptide consists of 1367 amino acid moieties, carrying two sets of Walker A, Walker B (Walker et al., 1982), and signature C (Higgins, 1992) motifs within the peptide (Fig. 2A). Based on the ATP binding cassettes and the putative trans-membrane spanning domains (Fig. 2B), Abcc12 is regarded as a 'full' ABC protein. The amino acid sequence of the Abcc12 protein deduced from the cloned cDNA exhibits the highest identity (84.5%) to human ABCC12 among all of the members of the ABCC subfamily hitherto identified in the human and the mouse (Table 1 and Fig. 3). Indeed, the hydropathy profile of mouse Abcc12 is virtually the same as that of human ABCC12 (Fig. 2B). From these results, it could be concluded that mouse Abcc12 is the orthologue of human ABCC12. In addition, our data suggest that the cDNA sequence of human ABCC12 (MRP9) recently reported by Bera et al. (2002) may be a splicing variant form, since exons 5 and 16 are missing in their sequence.

Based on the phylogenic relationship deduced from the amino acid sequence identities, the ABCC subfamily could be clustered into four classes (Fig. 3). For example, class A involves human ABCC1, ABCC2, ABCC3, and ABCC6, as well as mouse Abcc1, Abcc2, and Abcc6. These ABC transporters appear to function as conjugate transporters, e.g., GS-X pumps and/or multi-specific organic anion transporters (cMOAT) (Ishikawa, 1992; Borst and Oude Elferink, 2002). On the other hand, class B includes human ABCC8 (SUR1), ABCC9 (SUR2), and mouse Abcc9, which are sulfonylurea receptors coupled with potassium channels, i.e., Kir 6.1 or Kir 6.2. Human CFTR (ABCC7), ABCC10, mouse Abcc7 (mouse CFTR), and Abcc10 are involved in class C. Mutations in the *CFTR* gene are known to be the cause of cystic fibrosis, an autosomal recessive genetic disorder affecting a number of organs, including the lungs, airways, pancreas, and sweat glands (http://www.genet.sickkid.on.ca/cftr/). The physiological function of ABCC10 in this class is not known at the present time.

According to this clustering, the mouse Abcc12 belongs to class D, which involves human ABCC4, ABCC5, ABCC11, and ABCC12, as well as mouse Abcc4 and Abcc5 (Fig. 3). Recent studies demonstrated that human both ABCC4 and ABCC5 transport nucleotide analogues (Schuetz et al., 1999; Wijnholds et al., 2000; Jedlitschky et al., 2000; Chen et al., 2001). ABCC5 reportedly does not confer multidrug resistance when over-expressed in human embryonic kidney 293 cells (McAleer et al., 1999). Because of the similarity of the amino acid sequences, it is assumed that human ABCC11 and ABCC12 are functionally related to ABCC4 or ABCC5.

4.2. Mouse Abcc12 gene: an orthologue of human ABCC12 gene

Our conclusion that mouse Abcc12 is the orthologue of human ABCC12 is supported by similarities in the location and organization of those genes, as well. The present study provides evidence that the open reading frame in the mouse Abcc12 cDNA consists of 29 exons, as does the human ABCC12 cDNA (Yabuuchi et al., 2001; Tammur et al., 2001). In addition, the mouse *Abcc12* and human *ABCC12* genes (29 exons and introns) span 62 and 63 kb, respectively. The mouse *Abcc12* gene is located between two microsatellite markers, D8Mit347 and D8Mit348, on the chromosome 8D3 locus. This locus reportedly contains many conserved linkage homologies with human chromosome 16q12.1 (Serikawa et al., 1998), where the human *ABCC12* gene has recently been discovered (Yabuuchi et al., 2001; Tammur et al., 2001). Being consistent with this idea, the chromosomal location of the mouse *Siah 1* gene and its distance (167 kb) from the Abcc12 gene is conserved in the human chromosome 16q12.1 where both *SIAH 1* and *ABCC12* genes are located. The human *SIAH 1* gene (Hu et al., 1997) encodes a 282-amino-acid protein with 76% amino acid identity to the *Drosophila* SINA protein which is involved in the *ras* signaling pathway to mediate the R7 photoreceptor formation in the *Drosophila* eye (Carthew and Rubin, 1990). *Siah 1a* is one of the mouse orthologue genes and is mapped on the chromosome 8D3 locus (Holloway et al., 1997). Taken together, it is strongly suggested that the mouse *Abcc12* gene is closely related to the human *ABCC12* gene in terms of both the protein structure and the organization of the gene.

It is of importance, however, to note that in spite of the tandem location of both *ABCC11* and *ABCC12* genes on human chromosome 16q12.1, there was no mouse orthologue gene corresponding to the human *ABCC11* at that mouse chromosomal locus. In addition, there was no putative *Abcc11* gene detected even by an extensive search throughout the currently available mouse genome data. Thus, it appears that the *Abcc11* gene is absent from the mouse genome.

4.3. Tissue-specific expression of the mouse Abcc12 gene

We have previously reported that the expression of the

human *ABCC12* gene was widely distributed in various tissues, including testis, brain, liver, lung, kidney, thymus, prostate, ovary, colon, and leukocytes as well as in several fetal tissues (Yabuuchi et al., 2001). In contrast, the present study demonstrates that the mouse *Abcc12* gene is expressed at high levels exclusively in the testis (Fig. 5). The reason for such differences in organ-specific expression profiles between mouse Abcc12 and human ABCC12 is not known, but may be eventually explained by analysis of the promoter regions of those genes.

In the present study, by means of laser-captured microdissection combined with RT–PCR as well as in situ hybridization, the *Abcc12* transcript was detected in Sertoli cells of the seminiferous tubules in the mouse testis (Fig. 6A,B). In addition, in situ hybridization further revealed the expression of the *Abcc12* in Leydig cells, as well (Fig. 6B). Accumulating evidence suggests that the blood-testis barrier plays an important role in protecting the germ cells from harmful influences. To date it has been reported that ABCB1 (P-glycoprotein or MDR1) is expressed in luminal capillary endothelium and on the myoid-cell layer around the seminiferous tubule (Bart et al., 2002), whereas ABCC1 (MRP) is located basolaterally on both Sertoli and Leydig cells (Wijnholds et al., 1998). These ABC transporters are regarded as the first line players in the body's detoxification system. In this context, Abcc12 is also considered to play a role as a member of such a detoxification system, or it may be involved in the transport of endogenous substances in the testis. The physiological function and substrate specificity of Abcc12 remains to be elucidated.

4.4. Concluding remarks

Northern blot analysis revealed that mRNA with a size of 5.4 kb is the major transcript of mouse Abcc12 in the testis (Fig. 5B). In the present study, however, we have detected the existence of at least two splice variants for mouse Abcc12 (Fig. 7). In addition, the results of the FANTOM 2 project (The FANTOM Consortium, 2002) demonstrate that there is another splicing variant form that encodes a shorter peptide of Abcc12 (Fig. 7). These data suggests that mouse Abcc12 is transcribed into multiple forms by means of alternative splicing.

In the previous paper, we demonstrated that the human ABCC12 gene is transcribed into several splice variants (Yabuuchi et al., 2001). Recently, Bera et al. (2002) reported that the human ABCC12 (MRP9) is expressed as two major transcripts of 4.5 and 1.3, and that the 4.5 kb transcript is highly expressed in the epithelial cells of breast cancer. Transcript of the ABCC12 gene were detected in cell lines of carcinoma and adenocarcinoma originating from breast, lung, colon pancreas and prostate, as well (Yabuuchi et al., 2001), suggesting that expression of the ABCC12 gene may be up-regulated during carcinogenesis. Therefore, it is of great interest to study how alternative splicing is regulated in the expression of the human ABCC12 and mouse Abcc12 genes.

Acknowledgements

The authors thank Ms. Yukiko Saito (University of Tokyo Medical School) for her technical assistance in the preparation of tissue samples. This study was supported by research grants entitled 'Studies on the genetic polymorphism and function of pharmacokinetics-related proteins in Japanese population' (H12-Genome-026) and 'Toxicoproteomics: expression of ABC transporter genes and drug–drug interactions' (H14-Toxico-002) from the Japanese Ministry of Health and Welfare as well as by a Grant-in-Aid for Creative Scientific Research (No. 13NP0401) and a research grant (No. 14370754) from the Japan Society for the Promotion of Science. In addition, this study was supported, in part, by the institutional core grant of the 21st Century COE Program from the Ministry of Education, Culture, Sports, Science and Technology.

References

Bart, J., Groen, H.J.M., van der Graaf, W.T.A., Hollema, H., Hendrikse, N.H., Vaalburg, W., Sleijfer, D.T., de Vries, E.G.E., 2002. An oncological view on the blood-testis barrier. Lancet Oncol. 3, 357–363.

Bera, T.K., Lee, S., Salvatore, G., Lee, B., Pastan, I., 2001. MRP8, a new member of ABC transporter superfamily, identified by EST database mining and gene prediction program, is highly expressed in breast cancer. Mol. Med. 7, 509–516.

Bera, T.K., Iavarone, C., Kumar, V., Lee, S., Lee, B., Pastan, I., 2002. MRP9, an unusual truncated member of the ABC transporter superfamily, is highly expressed in breast cancer. Proc. Natl. Acad. Sci. USA 99, 6997–7002.

Borst, P., Oude Elferink, R., 2002. Mammalian ABC transporters in health and disease. Annu. Rev. Biochem. 71, 537–592.

Carninci, P., Kvam, C., Kitamura, A., Okazaki, Y., Kamiya, M., Shibata, K., Sasaki, N., Izawa, M., Muramatsu, M., Hayashizaki, Y., Schneider, C., 1996. High-efficiency full-length cDNA by biotinylated CAP trapper. Genomics 37, 327–336.

Carthew, R.W., Rubin, G.M., 1990. Seven in absentia, a gene required for specification of R7 cell fate in the Drosophila eye. Cell 63, 561–577.

Chen, Z.S., Lee, K., Kruh, G.D., 2001. Transport of cyclic nucleotides and estradiol 17-beta-D-glucuronide by multidrug resistance protein 4. Resistance to 6-mercaptopurine and 6-thioguanine. J. Biol. Chem. 276, 33747–33754.

Cole, S.P., Bhardwaj, G., Gerlach, J.H., Mackie, J.E., Grant, C.E., Almquist, K.C., Stewart, A.J., Kurz, E.U., Duncan, A.M., Deeley, R.G., 1992. Overexpression of a transporter gene in a multidrug-resistant human lung cancer cell line. Science 258, 1650–1654.

Dean, M., Rzhetsky, A., Allikmets, R., 2001. The human ATP-binding cassette (ABC) transporter superfamily. Genome Res. 11, 1156–1166.

Higgins, C.F., 1992. ABC transporters: from microorganisms to man. Annu. Rev. Cell Biol. 8, 67–113.

Holloway, A.J., Della, N.G., Fletcher, C.F., Largespada, D.A., Copeland, N.G., Jenkins, N.A., Bowtell, D.D., 1997. Chromosomal mapping of five conserved murine homologs of the Drosophila RING finger gene Seven-in-absentia. Genomics 41, 160–168.

Hu, G., Chung, Y.-L., Glover, T., Valentine, V., Look, A.T., Featon, E.R.,

1997. Characterization of human homologs of the Drosophila seven in absentia (sina) gene. Genomics 46, 103–111.

Ishikawa, T., 1989. ATP/Mg^{2+}-dependent cardiac transport system for glutathione S-conjugates: A study using rat heart sarcolemma vesicles. J. Biol. Chem. 264, 17343–17348.

Ishikawa, T., 1992. The ATP-dependent glutathione S-conjugate export pump. Trends Biochem. Sci. 17, 463–468.

Ishikawa, T., 2003. Multidrug resistance: genomics of ABC transporters. Encyclopedia of Human Genome, Nature Publishing Group, in press.

Jedlitschky, G., Burchell, B., Keppler, D., 2000. The multidrug resistance protein 5 functions as an ATP-dependent export pump for cyclic nucleotides. J. Biol. Chem. 275, 30069–30074.

Klein, I., Sarkadi, B., Varadi, A., 1999. An inventory of the human ABC proteins. Biochim. Biophys. Acta 1461, 237–262.

Kozak, M., 1991. An analysis of vertebrate mRNA sequences: intimations of translational control. J. Cell Biol. 115, 887–903.

Kyte, J., Doolittle, R.F., 1982. A simple method for displaying the hydropathic character of a protein. J. Mol. Biol. 157, 105–132.

Lee, W.-L., Tay, A., Ong, H.-T., Goh, L.-M., Monaco, A.P., Szepetowski, P., 1998. Association of infantile convulsions with paroxysmal dyskinesias (ICCA syndrome): confirmation of linkage to human chromosome 16p12–q12 in a Chinese family. Hum. Genet. 103, 608–612.

Leier, I., Jedlitschky, G., Buchholtz, U., Cole, S.p.C., Deeley, R.G., Keppler, D., 1994. The MRP encodes an ATP-dependent export pump of leukotriene C4 and structurally related conjugates. J. Biol. Chem. 269, 27807–27810.

McAleer, M.A., Breen, M.A., White, N.L., Matthews, N., 1999. pABC11 (also known as MOAT-C and MRP5), a member of the ABC family of proteins, has anion transporter activity but does not confer multidrug resistance when overexpressed in human embryonic kidney 293 cells. J. Biol. Chem. 274, 23541–23548.

Mouse Genome Sequencing Consortium, 2002. Initial sequencing and comparative analysis of the mouse genome. Nature 420, 520–562.

Müller, M., Meijer, C., Zaman, G.J., Borst, P., Scheper, R.J., Mulder, N.H., de Vries, E.G.E., Jansen, P.L.M., 1994. Overexpression of the gene encoding the multidrug resistance-associated protein results in increased ATP-dependent glutathione S-conjugate transport. Proc. Natl. Acad. Sci. USA 91, 13033–13037.

Saitou, N., Nei, M., 1987. The neighbor-joining method: a new method for reconstructing phylogenetic trees. Mol. Biol. Evol. 4, 406–425.

Schuetz, J., Connelly, M.C., Sun, D., Paibir, S., Flynn, P.M., Srinivas, R.V., Kumar, A., Fridland, A., 1999. MRP4: A previously unidentified factor in resistance to nucleoside-based antiviral drugs. Nature Med. 5, 1048–1051.

Serikawa, T., Cui, Z., Yokoi, N., Kuramoto, T., Kondo, Y., Kitada, K., Guenet, J.-L., 1998. A comparative genetic map of rat, mouse and human genomes. Exp. Anim. 47, 1–9.

Tammur, J., Prades, C., Arnould, I., Rzhetsky, A., Hutchinson, A., Adachi, M., Schuetz, J.D., Swoboda, K.J., Ptacek, L.J., Rosier, M., Dean, M., Allikmets, R., 2001. Two new genes from the human ATP-binding cassette transporter superfamily, ABCC11 and ABCC12, tandemly duplicated on chromosome 16q12. Gene 273, 89–96.

The FANTOM Consortium and the RIKEN Genome Exploration Research Group Phase I & II Team, 2002. Analysis of the mouse transcriptom based on functional annotation of 60,770 full-length cDNAs. Nature 420, 563–573.

Tomita, H., Nagamitsu, S., Wakui, K., Fukushima, Y., Yamada, K., et al., 1999. Paroxysmal kinesigenic choreoathetosis locus maps to chromosome 16p11.2–p12.1. Am. J. Hum. Genet. 65, 1688–1697.

Walker, J.E., Saraste, M., Runswick, M.J., Gay, N.J., 1982. Distantly related sequences in the α and β subunits of ATP synthetase, myosin, kinases and other ATP-requiring enzymes and a common nucleotide binding fold. EMBO J. 1, 945–951.

Wijnholds, J., Scheffer, G.L., van der Valk, M., van der Valk, P., Beijnen, J.H., Scheper, R.J., Borst, P., 1998. Multidrug resistance protein 1 protects the oropharyngeal mucosal layer and the testicular tubules against drug-induced damage. J. Exp Med. 188, 797–808.

Wijnholds, J., Mol, C.A., van Deemter, L., de Haas, M., Scheffer, G.L., Baas, F., Beijnen, J.H., Scheper, R.J., Hatse, S., De Clercq, E., Balzarini, J., Borst, P., 2000. Multidrug-resistance protein 5 is a multispecific organic anion transporter able to transport nucleotide analogs. Proc. Natl. Acad. Sci. USA 97, 7476–7481.

Yabuuchi, H., Shimizu, H., Takayanagi, S., Ishikawa, T., 2001. Multiple splicing variants of two new human ATP-binding cassette transporters, ABCC11 and ABCC12. Biochem. Biophys. Res. Commun. 288, 933–939.

Yabuuchi, H., Takayanagi, S., Yoshinaga, K., Taniguchi, N., Aburatani, H., Ishikawa, T., 2002. ABCC13, an unusual truncated ABC transporter, is highly expressed in fetal human liver. Biochem. Biophys. Res. Commun. 299, 410–417.

J Nutr Sci Vitaminol. 49, 125–132, 2003

Analysis of the Comprehensive Effects of Polyunsaturated Fatty Acid on mRNA Expression Using a Gene Chip

Yoko FUJIWARA[1,2], Masayo YOKOYAMA[1], Rumi SAWADA[1], Yousuke SEYAMA[1], Masami ISHII[3], Shunichi TSUTSUMI[3], Hiroyuki ABURATANI[3], Satoko HANAKA[2,4], Hiroshige ITAKURA[2,5] and Akiyo MATSUMOTO[2,6,*]

[1] *Department of Food Science and Nutrition, Ochanomizu University, Tokyo 112–8610, Japan*
[2] *Division of Clinical Nutrition, National Institute of Nutrition and Health, Tokyo 162–8636, Japan*
[3] *Genome Sciences, Research Center for Advanced Science and Technology, The University of Tokyo, Tokyo, Japan*
[4] *Medical School of Teikyo University, Tokyo 153–8904, Japan*
[5] *Department of Life Science, Ibaraki Christian University, Ibaraki, Japan*
[6] *Department of Clinical Dietetics and Human Nutrition, Josai University, Saitama 350–0295, Japan*

(Received October 3, 2002)

Summary To investigate the comprehensive effects of polyunsaturated fatty acids (PUFA) on gene expression, we analyzed changes of mRNA expression in PUFA-treated HepG2 cells using a DNA micro array. We incubated HepG2 cells for 24 h with or without 0.25 mM oleic acid (OA), arachidonic acid (AA), eicosapentaenoic acid (EPA) or docosahexaenoic acid (DHA), and then compared the expression profiles of thousands of genes using a GeneChip. PUFA influenced the expression of various genes related to cell proliferation, growth and adhesion, as well as for many transcription factors including sterol regulatory element binding proteins (SREBP). Treatments with AA, EPA, and DHA repressed the expression of genes related to cholesterol and lipid metabolism. Moreover, data from gene chip analysis proved that PUFA reduced the expression of prostasin, which is a serine protease. By measuring the mRNA levels of SREBPs, mevalonate pyrophosphatase and prostasin using quantitative RT-PCR, we confirmed the effect of PUFA revealed by gene chip analysis. These data might provide useful clues with which to explore novel functions of PUFA.

Key Words DNA micro array, polyunsaturated fatty acid, HepG2 cells

Fatty acids (FA) are important not only as an energy source but also as components of the cell membrane because fatty acid composition influences membrane fluidity and the function of receptors or channels (*1*). Polyunsaturated fatty acids (PUFA) decrease plasma triacylglycerols and cholesterol levels and influence lipid metabolism (*2*). Many studies within the past decade have shown that PUFA function as mediators of gene transcription. One of the mechanisms is explained by the down-regulation of the sterol regulatory element binding protein (SREBP), which regulates the intracellular cholesterol metabolism (*3*, *4*). On the other hand, peroxisome proliferator activated receptor (PPAR), which binds FA and its metabolites, regulates the gene expression concerned with the β-oxidation of fatty acids (*5*). Several other factors such as liver X receptor (LXR) (*6*), hepatocyte nuclear factor 4 (HNF4) (*7*), *c-fos* and *nur-77* (*8*) are also thought to regulate the expression of genes that respond to FA.

The mechanism of how PUFA controls gene expression was summarized as follows (*9*). Fatty acids or their derivatives function as ligands for a transcription factor (TF), which then binds DNA at the FA response element and activates or represses transcription. Fatty acids or their derivatives thereby modify transcriptional potency and initiate a signal transduction cascade to induce covalent modification of a TF. Fatty acids act indirectly via

* To whom correspondence should be addressed.
E-mail: amatsu@josai.ac.jp

Abbreviations: AA, arachidonic acid; ACAT, acyl CoA: cholesterol acyltransferase; BSA, bovine serum albumin; CETP, cholesteryl ester transfer protein; DHA, docosahexaenoic acid; DMEM, Dulbecco's modified Eagle's medium; EPA, eicosapentaenoic acid; FA, fatty acid; HNF4, hepatocyte nuclear factor 4; HTGL, hepatic triglyceride lipase; LCAT, lecithin-cholesterol acyltransferase; LPDS, lipoprotein-deficient serum; LXR, liver X receptor; MPD, mevalonate pyrophosphate decarboxylase; OA, oleic acid; PPAR, peroxisome proliferator activated receptor; PUFA, polyunsaturated fatty acids; ROS, reactive oxygen species; RT-PCR, reverse transcriptase-polymerase chain reaction; SA, stearic acid; SDS, sodium dodecyl sulfate; SRE, sterol regulatory element; SREBP, sterol regulatory element-binding protein; SSPE, buffer consisting of saline, sodium dihydrogen phosphate-ethylenediamine tetraacetate.

alterations in either TF mRNA stability or gene transcription, resulting in variations of de novo TF synthesis with impact on the transcription rate of genes encoding proteins related to FA transport and metabolism (*9*).

Despite much recent progress, the mechanism(s) by which FA modulate gene transcription remains largely unknown. DNA micro array is known to be a powerful tool to investigate mRNA expression profiles, and has been widely applied in the field of drug innovation to analyze functions and side effects of new compounds. In this study, to investigate the comprehensive effects of PUFA on gene regulation, we analyzed mRNA expression profiles in PUFA-treated HepG2 cells using a DNA micro array.

MATERIALS AND METHODS

Cell culture with fatty acids. The human hepatoma cell line, HepG2, purchased from the Riken Gene Bank (Tsukuba, Japan) was cultured in Dulbecco's modified Eagle's medium (DMEM) supplemented with 10% fetal calf serum (Intergen Co., Purchase, NY, USA) at 37°C under a 5% CO_2 atmosphere. Cells seeded in 60-mm diameter collagen-coated culture dishes (Sumitomo Bakelite Co., Ltd., Tokyo, Japan) at a density of 1×10^6/dish were cultured to approximately 90% confluence and then incubated with 0.25 mM oleic acid (18 : 1, OA), arachidonic acid (20 : 4, AA), eicosapentaenoic acid (20 : 5, EPA) or docosahexaenoic acid (22 : 6, DHA) in DMEM supplemented with 10% fetal calf lipoprotein-deficient serum (LPDS), which eliminates FA in the serum (all from Sigma-Aldrich Chemical Co., St Louis, MO, USA). The FAs were dissolved in essential FA-free bovine serum albumin (BSA). Control HepG2 cells were incubated with the same 10% LPDS/DMEM without FA. After a 24-h incubation at 37°C, the cells were harvested. Total RNA was isolated from the cells using a RNeasy Mini Kit (Qiagen Inc., Valencia, CA, USA) according to the manufacturer's instructions. Cells were pooled from triplicate dishes and then poly(A)$^+$ RNA was purified using a QuickPrep micro mRNA purification kit (Amersham Pharmacia Biotech Inc., Piscataway, NJ, USA).

Micro array analysis of expression profiles. Studies using the GeneChip proceeded according to the technical manual supplied with the Affymetrix GeneChip Expression Analysis System (*10, 11*). First-strand cDNA was generated with 1 μg of poly(A)$^+$ RNA and 0.1 μmol of T7-linked oligo(dT)$_{24}$ primer (Amersham Pharmacia Biotech Inc.) using SuperScript Choice System (Life Technologies, Rockville, MD, USA). After second-strand synthesis, in vitro transcription was performed using biotinylated UTP and CTP (Enzo Diagnostics, Inc., Farmingdale, NY, USA). The amplified cRNA was purified by passage through a column containing affinity resin (RNeasy Mini Kit, Qiagen Inc.), and quantified by absorbance at 260 nm. Biotinylated cRNA (25 μg) was fragmented into 50- to 150-nt units before overnight hybridization to GeneChips (HuGene FL Array, Affymetrix Inc., Santa Clara, CA, USA) that contain oligonucleotide probe sets for approximately 6,000 human genes. Fragmented cRNA and sonicated herring sperm DNA, up to 0.1 mg/mL, were added to hybridization buffer containing 1 M NaCl, 10 mM Tris-HCl (pH 7.6), and Triton X-100 (ST-T). The mixture was denatured at 99°C for 5 min, incubated at 45°C for 5 min, and then a hybridization cocktail was injected into the probe array cartridge. Hybridization proceeded at 45°C for 16 h with rotary shaking at 60 rpm. Thereafter, the hybridization solution was removed from the array, which was filled with non-stringent washing buffer (5×SSPE, 0.01% Tween-20, 0.05% antifoam). The hybridized array was stained with 5.0 μg/mL streptavidin/phycoerythrin (Molecular Probes, Eugene, OR, USA) and 2.0 mg/mL acetylated BSA (Sigma, St. Louis, MO, USA) in 1×ST-T at 40°C for 15 min. The probe array was scanned twice at 3 μm of resolution using an HP GeneArray Scanner (Affymetrix Inc.).

The intensity of each feature of the array was captured by Affymetrix GeneChip Software (Affymetrix Inc.) according to standard Affymetrix procedures (*10, 11*) with a class AB mask file. This file is designed to exclude inappropriate probe pairs that represent introns or reverse sequences. A single expression level for each gene was derived from 20 probe pairs representing each gene, that is, ~20 perfectly matched (PM) and mismatched (MM) control probes. The MM probes act as specific controls that allow the direct subtraction of background and cross-hybridization signals. The average difference (Avg. diff.) representing PM−MM for each gene-specific probe set shows the quantitative mRNA levels. The fold change of the transcripts between the control and the experimental sample was calculated as follows:

$$\text{Fold change} = \{\text{Avg. diff. change}/\max[\min(\text{Avg. diff.}_{\text{exp.}}, \text{Avg. diff.}_{\text{control}}), Q_M * Q_C]\} + (+1 \text{ if Avg. diff.}_{\text{exp.}} \geq \text{Avg. diff.}_{\text{control}} \; -1 \text{ if Avg. diff.}_{\text{exp.}} \leq \text{Avg. diff.}_{\text{control}})$$

Where

$$\text{Avg. diff. change} = \text{Diff.}_{\text{exp.}} - \text{Avg. diff.}_{\text{control}}$$

$$Q_C = \max(Q_{\text{exp.}}, Q_{\text{control}})$$

And the Q multiplier

Q_M = 2.1 in 50 μm feature arrays and 2.8 in 24 μm feature arrays.

This equation permits the expression of fold change as a positive number when the transcript increased over its control state, and as a negative number when the transcript level decreased. If the noise ($Q\ Q_M$) of either array was greater than the Avg. diff. of the transcript (in either the control or experimental data), the fold change was calculated using the noise.

Quantitative RT-PCR. Single-strand cDNA was synthesized from 1 μg of total RNA using random hexamer and TaqMan Reverse Transcription Reagents (Applied Biosystems, Foster City, CA, USA). Primers for PCR were designed using Primer Express (Applied Biosystems) software. Primer sequences were 5′-GCAAGGCCATCG-

ACTACATTC-3′ (forward) and 5′-TTGCTTTTGTGGAC-AGCAGTG-3′ (backward) for SREBP-1; 5′-AGGCGGA-CAACCCATAATATCA-3′ (forward) and 5′-GACTTGTG-CATCTTGGCGTCT-3′ (backward) for SREBP-2; 5′-CGA-GTCACACTGGCCTGAACT-3′ (forward) and 5′-CACGG-TACTGCCTGTCAGCTT-3′ (backward) for MPD; 5′-CTT-GATCTTTGAGCCCATTCTTC-3′ (forward) and 5′-TCT-GGCCATTGCTACAGGC-3′ (backward) for prostasin; 5′-TTCAGAAAACACAGATGACCTACTACTTC-3′ (forward) and 5′-CTGATCTTTCGCTTTGATGTTTTAGAC-3′ (backward) for hepatic triglyceride lipase (HTGL); 5′-AAATT-CCATGGCACCGTCA-3′ (forward) and 5′-AGCATCGCC-CCACTTGATT-3′ (backward) for GAPDH. Real-time quantitative RT-PCR proceeded in a reaction mixture containing 10 ng of first-strand cDNA, 300 nM of each primer set in a final volume of 25 μl and SYBR Green PCR core reagent (Applied Biosystems). The results were analyzed using a GeneAmp 5700 sequence detection system (Applied Biosystems). All values were expressed as mean±SD. Significance of the difference between PUFA treatments ($p<0.05$) was determined by analysis of variance (ANOVA) using a Stat View software (Abucas Concepts, Inc., Berkeley, CA, USA).

RESULTS

Gene chip analysis

Table 1 shows the effect of FA on genes except for those related to cholesterol and lipoprotein metabolism. PUFA suppressed the mRNA levels of SREBPs, as well as of those expressing transcription factors such as NF-κB p65, nuclear factor I-X (NFI-X), PPARs and Rad2. PUFA repressed the expression of lipogenic genes such as fatty acid synthase and stearoyl-CoA desaturase. Although gene expression related to FA oxidation was not changed, PUFA up-regulated 2-oxoglutarate dehydrogenase, isocitrate dehydrogenase and succinyl-CoA synthetase, all of which are involved in the TCA cycle. However, the expression of LXR, HNF, *c-fos*, and *nur-77*, which were thought to responde to FA, did not change. All FA largely increased mRNA levels of metallothionein-IG, ventricular/slow twitch myosin alkali light chain (MLC-1V/Sb isoform), and deleted split hand/split foot 1 (DDS1). In addition, PUFA affected the expression of genes involved in cell differentiation and proliferation.

Table 2 shows changes in genes related to cholesterol and lipoprotein metabolism by FA treatments. PUFA suppressed the mRNA levels of LDL receptor, HMG CoA synthase and HMG CoA reductase, all of which are SREBP targets (*12–14*). Furthermore, the expression of mevalonate pyrophosphate decarboxylase (MPD) and squalene epoxidase, which function in the cholesterol synthetic pathway were down regulated. Lysosomal acid lipase was one of the PUFA responsive genes that had not been reported. Results of gene chip showed no change of the expression of LXR-alpha and undetectable levels of the mRNA expression of acyl CoA: cholesterol acyltransferase (ACAT), and cholesteryl ester transfer protein (CETP), which are thought to be regulated by PUFA (*15, 16*).

Quantitative RT-PCR

To confirm the effects of PUFA observed by DNA micro array analysis, we measured the mRNA levels of SREBPs and MDP in PUFA-treated HepG2 cells using real-time RT-PCR. AA, EPA, and DHA reduced the mRNA levels of SREBP-1 and -2, whereas OA did not affect the mRNA levels (Fig. 1). Generally, *n*-6 and *n*-3 PUFA similarly affect the expression level of SREBP. Figure 2 shows that PUFA also decreased the mRNA levels of MPD by 50%. We also confirmed the effect of PUFA on the mRNA levels of prostasin (Fig. 3). PUFA repressed the expression of prostasin, but changes in the mRNA levels were smaller than those shown by gene chip analysis. Figure 4 shows up-regulation by PUFA on the mRNA expression of HTGL.

DISCUSSION

The present study investigated the extensive effects of PUFA on gene expression in HepG2 cells and explored thenovel functions of PUFA. Few genes were induced or reduced by PUFA more than 8-fold among the approximately 6,000 gene probes on the oligonucleotide chip. The effects of PUFA on gene expression were moderate compared with those elicited by other drugs or chemicals (*17, 18*). This may be because PUFA are nutrients that are naturally catabolized to produce energy. As the MPD mRNA level was decreased by −9.5 (11%) with DHA by gene chip analysis, we measured the mRNA levels of MPD using a real time RT-PCR of HepG2 cells incubated with PUFA. The gene chip analysis showed reduced mRNA levels by −1.7, −1.2, −1.8 in SREBP-1, and −1.5, −1.9, −1.7 in SREBP-2 with AA, EPA, and DHA, respectively. We also analyzed mRNA levels of SREBPs in FA-treated HepG2 cells using quantitative RT-PCR (Fig. 1). We confirmed that PUFA suppressed MPD, and SREBPs but the magnitude of the effect was not equivalent between the data obtained from the gene chip analysis and that from RT-PCR. However, the gene chip analysis reflects the tendencies of PUFA, and is a useful tool for investigating the comprehensive effect. In the tables, therefore, we listed the data obtained using the gene chip with the absolute value of the fold change >2 and the similar tendencies among PUFA treatments.

The results of gene chip analysis showed the changes of SREBP and PPAR resulting from PUFA, but the analysis did not detect changes in HNF, *c-fos* and *nur-77*, which have been previously reported (*8*). More detailed measurements of each gene are required to accurately quantify changes in the mRNA levels. It may be related to the expression levels of some genes in HepG2 cells. Although HepG2 cells are familiar for investigating the lipid metabolism, the expression of PPAR was low whereas the expressions of apolipoproteins AI, AII, and E were high (data not shown).

Our data showed that PUFA repressed the expression of hepatic lipogenic genes and almost all of the genes associated with the cholesterol synthetic pathway. In this study using HepG2 cells, one of the major mechanisms of mRNA expression down-regulation caused by PUFA